



# Effectiveness of short term air quality emission controls: A high-resolution model study of Beijing during the APEC period

Tabish Umar Ansari<sup>1</sup>, Oliver Wild<sup>1</sup>, Jie Li<sup>2</sup>, Ting Yang<sup>2</sup>, Weiqi Xu<sup>2,3</sup>, Yele Sun<sup>2,3,4</sup>, and Zifa Wang<sup>2</sup>

<sup>1</sup>Lancaster Environment Centre, Lancaster University, UK

<sup>2</sup>State Key Laboratory of Atmospheric Boundary Layer Physics and Atmospheric Chemistry, Institute of Atmospheric Physics, Chinese Academy of Sciences, Beijing, China

<sup>3</sup>College of Earth Sciences, University of Chinese Academy of Sciences, Beijing, China

<sup>4</sup>Center for Excellence in Regional Atmospheric Environment, Institute of Urban Environment, Chinese Academy of Sciences, Xiamen, China

Correspondence to: Tabish Umar Ansari (t.ansari@lancaster.ac.uk)

**Abstract.** We explore the impacts of emission controls on haze events in Beijing in October–November 2014 using high resolution WRF-Chem simulations. The model reproduces surface temperature and relative humidity profiles over the period well and captures the observed variations in key atmospheric pollutants. We highlight the sensitivity of simulated pollutant levels to meteorological variables and model resolution, and in particular to treatment of turbulent mixing in the planetary boundary layer. We note that simulating particle composition in the region remains a challenge, and we overpredict NH<sub>4</sub> and NO<sub>3</sub> at the expense of SO<sub>4</sub>. We find that the emission controls implemented for the APEC Summit period made a relatively small contribution to improved air quality (20–26%), highlighting the important role played by favourable meteorological conditions over this period. We demonstrate that the same controls applied under less favourable meteorological conditions would have been insufficient to reduce pollutant levels to meet the required standards. Continued application of these controls over the 6-week period considered would only have reduced the number of haze days where daily-mean fine particulate matter exceeds 75 µg m<sup>-3</sup> from 15 to 13 days. Our study highlights the limitations of current emission controls and the need for more stringent measures over a wider region during meteorologically stagnant weather.

*Copyright statement.*

## 1 Introduction

Air pollution poses serious health risks to urban residents and is one of the most important environmental problems facing cities around the world (Liang et al., 2017). Fine particulate matter with a diameter less than 2.5 µm (PM<sub>2.5</sub>) is a major air pollutant that often exceeds safe limits during haze episodes which are a common occurrence in many developing megacities over the past decade. It is estimated that a 10 µg m<sup>-3</sup> decrease in PM<sub>2.5</sub> concentration is related to an increase in mean life expectancy of as much as 0.6 years (Pope et al., 2009). PM<sub>2.5</sub> also reduces visibility and has important impacts on regional climate (Westervelt et al., 2016). Beijing is the capital, political and cultural center of China and is among the most polluted



cities in the country (Batterman et al., 2016). The population of Beijing municipality increased from 14.2 million in 2002 to 21.2 million in 2013 (Ma et al., 2014) and this has been accompanied by an increase in anthropogenic emissions across the region. High  $\text{PM}_{2.5}$  concentrations are frequently reported in city clusters in the Beijing-Tianjin-Hebei, Yangtze River Delta, and Pearl River Delta regions in China. Haze episodes are particularly common during winter months and have attracted substantial scientific attention (Gao et al., 2017). Independent observational (Gao et al., 2016a; Zhong et al., 2018; Shang et al., 2018; Chen et al., 2015b; Sun et al., 2016a) modelling (Matsui et al., 2009; Kajino et al., 2017; Gao et al., 2015a; Chen et al., 2016a) and long-term data analysis studies (Chen et al., 2016b; Liu et al., 2016b; Chen et al., 2015a; Yan et al., 2018) have investigated the sources, evolution and fate of  $\text{PM}_{2.5}$  in Beijing, but many uncertainties remain, and improved understanding is required in order to inform sound, evidence-based emission control policies. Strict short-term emission controls have been applied effectively to improve air quality in Beijing during the Beijing Olympics in 2008 (Gao et al., 2011; Yang et al., 2011) and more recently for major events such as the Asia-Pacific Economic Cooperation (APEC) summit in November 2014 (Li et al., 2017b; Wang et al., 2016b) and the Victory Parade in 2015 (Liang et al., 2017; Liu et al., 2016a; Zhao et al., 2017). Real-world emission controls provide an ideal opportunity to test current scientific understanding of the sources and processing of air pollution as represented in models in a robust way. With improved confidence in model performance over a focus region we can explore the impact of alternative control options to aid formulation of more effective policies for emission reduction.

A number of previous studies have investigated the effect of emission controls during the APEC period in November 2014 using surface observations (Sun et al., 2016b; Xu et al., 2015; Wang et al., 2016b; Li et al., 2017b; Zhou et al., 2017) and atmospheric chemical transport models (Zhang et al., 2016; Guo et al., 2016; Wang et al., 2017; Gao et al., 2017) and have found that  $\text{PM}_{2.5}$  concentrations were much lower than during the preceding weeks. Many of these studies have attributed this improved air quality largely to the emission controls that were applied without thoroughly evaluating the role of meteorological variations. Comparison with observations in preceding weeks or over similar time periods in earlier years does not adequately account for the role of meteorology in governing haze episodes. Model studies with and without emission controls are insufficient to evaluate the contribution of meteorological processes if they focus on the control period alone, without evaluating the model performance outside the control period. Gao et al. (2017) found that the emission controls reduced  $\text{PM}_{2.5}$  levels by about  $18 \mu\text{g m}^{-3}$  during APEC with about half the reduction due to emission controls in surrounding districts outside Beijing. However, the study involved coarse resolution (27 km) model simulations which may be insufficient to capture regional and city-level atmospheric events well, and lacked component level analysis of aerosols. Other studies have noted the role of meteorology during the period but have not quantified it, attributing the benefits mostly to emission controls.

In this study we investigate the effectiveness of short-term emission controls and how meteorological processes influence this, using the APEC period as an example. We use a nested version of the Weather Research and Forecasting model with Chemistry (WRF-Chem) over China with a specific focus on the Beijing-Tianjin-Hebei region. WRF-Chem has been used successfully at coarser resolution in previous studies investigating haze formation over Beijing (Matsui et al., 2009; Tie et al., 2014; Zhang et al., 2015; Chen et al., 2016a). We describe the model setup, emissions and observations in Section 2. In Section 3 we present a thorough meteorological and chemical evaluation of the model simulations against surface observations and tower measurements, including aerosol composition, and we assess the strengths and weaknesses of the model. We also test



different meteorological inputs to drive the model. We present sensitivity studies to model resolution, uncertainties in ammonia emissions and boundary layer processes in Section 4. In Section 5 we investigate the impact of emissions controls over the APEC period and compare these with the same controls over a period two weeks earlier to demonstrate the important role of meteorological conditions in governing their effectiveness.

## 5 2 Model configuration and the APEC period

We use the WRF-Chem model (Grell et al., 2005; Fast et al., 2006) version 3.7.1 to simulate the meteorology and air quality over Northern China. Previous studies have shown that WRF-Chem is capable of reproducing air quality in China relatively well (Gao et al., 2015a, 2016b; Guo et al., 2016; Chen et al., 2016a). We use the Carbon Bond Mechanism version-Z (CBMZ) chemistry scheme coupled with the Model of Simulating Aerosol Interactions and Chemistry (MOSAIC) aerosol module (Zaveri et al., 2008). CBMZ explicitly treats 67 species with 164 gas-phase, heterogeneous and aqueous reactions, and provides a suitable compromise between chemical complexity and computational efficiency. MOSAIC uses a sectional approach with eight aerosol size bins and treats the key aerosol species, including sulfate, nitrate, chloride, ammonium, sodium, black carbon (BC), primary organic mass, liquid water and other inorganic mass. Secondary organic aerosol (SOA) formation is not included in the chemical mechanism used here. While SOA may contribute as much as 17–23% to aerosol composition in the October–November period investigated here, it does not respond strongly to emission controls (Sun et al., 2016b). In contrast secondary inorganic aerosols contribute up to 62% by mass of total fine particulate matter over the North China Plain, and show a significant decrease in response to emission controls (Sun et al., 2016b), and our emphasis is largely on these components here.

Further details of the model configuration used in this study are given in Table 1. We perform two-way coupled simulations with three nested domains that include China as the parent domain (D01) at 27 km horizontal resolution, Northern China as a nest (D02) at 9 km resolution and the North China Plain as an innermost nest (D03) at 3 km resolution, as shown in Fig. 1. The model is nudged to meteorological reanalysis data above the boundary layer every six hours for winds, temperature and moisture to permit direct comparison of the simulations with observed pollutant concentrations under comparable conditions.

We use anthropogenic emissions from the Multi-resolution Emission Inventory for China (MEIC) for the year 2010 (Li et al., 2017c). This provides emissions of major air pollutants including  $\text{NO}_x$ , CO, NMVOC,  $\text{SO}_2$ ,  $\text{NH}_3$ ,  $\text{PM}_{2.5}$ ,  $\text{PM}_{10}$ , BC and OC from five major emission sectors that include residential, traffic, industry, power and agricultural sources, and has been used in a number of previous modelling studies (Li et al., 2015; Gao et al., 2015a; Zhang et al., 2015; Chen et al., 2015a, 2016a). Emissions were provided at the native resolution of each domain, i.e., at 27 km, 9 km and 3 km. We impose a vertical profile for these emissions over the lowest eight model levels to account for the effective source height distribution for each sector based on the distribution used for EMEP emissions (Bieser et al., 2011; Mailler et al., 2013), and impose a diurnal cycle for each source sector in the MEIC inventory.  $\text{SO}_2$  emissions over the Beijing-Tianjin-Hebei region were reduced by 50% to account for strong emission reductions between 2010 and our focus year of 2014 (Zheng et al., 2018). We assume that 6% by mass of  $\text{SO}_2$  is emitted as primary  $\text{SO}_4$  to account for the discrepancy between high observed concentrations of  $\text{SO}_4$  and low secondary production in the model (Gao et al., 2015a; Chen et al., 2016a; Li et al., 2017a). Biogenic emissions are based on

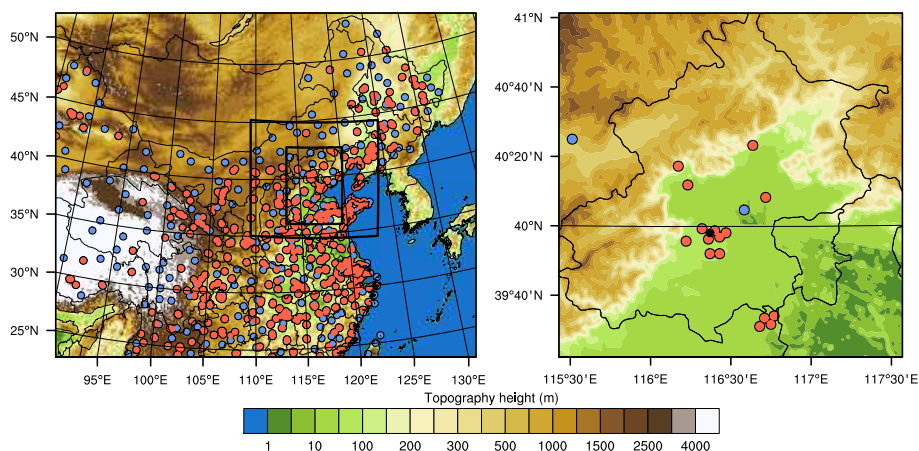


**Figure 1.** Map of topography over the model domain (left) showing nests over Northern China and the North China Plain, and map of Beijing municipality (right) showing the location of IAP (black) and measurement stations for meteorology (blue) and air quality (red).

**Table 1.** Model configuration used in this study

Configuration	Description
Horizontal resolution	27 km, 9 km, 3 km (3 domains)
Vertical levels	31 with model top at 50 hPa
Aerosol scheme	MOSAIC (8 bins) (Zaveri et al., 2008)
Photolysis scheme	Fast-J photolysis (Wild et al., 2000)
Gas-phase chemistry	CBMZ (Zaveri and Peters, 1999)
Cumulus parameterization	Grell 3-D scheme
Shortwave radiation	RRTMG shortwave scheme (Clough et al., 2005)
Longwave radiation	RRTMG longwave scheme (Mlawer et al., 1997)
Cloud Microphysics	Lin scheme (Lin et al., 1983)
Land surface scheme	NOAH LSM (Chen and Dudhia, 2001)
Land-use data	MODIS 20 category at 30 arcseconds
Surface layer scheme	Monin-Obukhov scheme (Monin and Obukhov, 1954)
Boundary layer scheme	YSU (Hong et al., 2006)
Meteorological conditions	ECMWF 6-hourly data
Chemical boundary conditions	MOZART (Emmons et al., 2010)

the Model of Emissions of Gases and Aerosols from Nature (MEGAN, Guenther et al., 2012). These are calculated online in the model based on canopy and emission factors and factors for leaf age, soil moisture, leaf area index, light dependence and



temperature responses. Hourly fire emissions are included from the Fire Emissions Inventory from NCAR (FINN, Wiedinmyer et al., 2011) to represent biomass burning, although this is not a major source in the region at this time of year.

To evaluate the model, meteorological observations were obtained from the National Climate Data Center (NCDC) hourly integrated surface database (<http://www.ncdc.noaa.gov/data-access/>) for all of China. These sites are shown in Fig. 1. We focus on 2 m temperature and relative humidity and 10 m wind speed and direction for model evaluation. Vertical profiles of meteorological variables were also obtained from the 325 m high observational tower located at the Institute of Atmospheric Physics (IAP), Chinese Academy of Sciences, Beijing (39°58'28" N, 116°22'16" E). This provides independent measurements of temperature, relative humidity, wind speed and wind direction at 17 different height levels. Measurements of boundary layer mixing height were retrieved from aerosol lidar profiles at IAP (Yang et al., 2017), providing a valuable additional test of model meteorological processes. Hourly concentrations of NO<sub>2</sub>, CO, SO<sub>2</sub>, O<sub>3</sub>, PM<sub>2.5</sub> and PM<sub>10</sub> are available from the national monitoring network run by the China National Environmental Monitoring Center (CNEMC). In addition, over the October–November 2014 period detailed measurements of atmospheric pollutants and aerosol composition were made from the IAP tower. These include measurements of NH<sub>4</sub>, NO<sub>3</sub>, SO<sub>4</sub>, and OC from an Aerodyne Aerosol Chemical Speciation Monitor (ACSM) instrument at 260 m altitude (Sun et al., 2016b) and from a High Resolution Aerosol Mass Spectrometer (HR-AMS) instrument at the surface (Xu et al., 2015), and BC at the surface was measured with an Aethalometer. The size-segregated samples collected at the two heights were analyzed for water-soluble ions. Detailed procedures for the data analysis are described in Ng et al. (2011) and Sun et al. (2012).

### 3 Model Evaluation

To investigate the strengths and weaknesses of the model in representing air quality in China, the model was evaluated against meteorological and pollutant measurements across all three domains and at the IAP tower site in Beijing.

#### 3.1 Meteorology

We test the model performance with two sets of meteorological fields: Final Reanalysis data (FNL) from the National Centers for Environmental Prediction (NCEP) and ERA-Interim data from the European Centre for Medium-Range Weather Forecasts (ECMWF). Table 2 presents a domain-based comparison of the performance of simulated meteorological variables with ground-based observations from the NCDC dataset when the model was run using these meteorological fields. With both sets of fields the average 2 m temperature is reproduced well over domains 2 and 3, but is slightly underpredicted over the largest domain, and is overpredicted for the single Beijing site. The Beijing observations are made at the airport on the outskirts of the city, and may not be representative of the wider region. The correlation coefficients are high over all three model domains (0.94–0.95) with both ECMWF and FNL fields. The surface relative humidity is underpredicted for all domains with both sets of fields, although the biases are smaller and correlation coefficients higher with ECMWF data. The humidity is underpredicted by about 15% at the Beijing site and this may have implications for heterogeneous reactions and the hygroscopic growth of secondary aerosols. The 10 m wind speed is substantially underpredicted with both sets of fields for all domains,



**Table 2.** Comparison of observed and simulated meteorological variables using FNL and ECMWF fields

	Number of Stations	Obs. avg.	Sim avg		Bias		RMSE		r	
			FNL	ECMWF	FNL	ECMWF	FNL	ECMWF	FNL	ECMWF
2-m Temperature (°C)										
Beijing	1	9.68	11.52	11.44	1.84	1.76	3.28	3.36	0.88	0.87
D03	30	8.91	8.98	8.95	0.07	0.04	2.47	2.46	0.94	0.94
D02	77	7.87	7.53	7.55	-0.34	-0.32	2.39	2.35	0.95	0.95
D01	324	9.62	7.77	7.79	-1.85	-1.83	3.23	3.23	0.94	0.94
2-m Relative Humidity (%)										
Beijing	1	54.7	34.1	39.1	-20.6	-15.6	26.9	22.4	0.77	0.81
D03	30	54.9	44.8	48.9	-10.1	-6.0	19.6	16.7	0.75	0.78
D02	77	54.4	47.8	51.1	-6.6	-3.3	17.4	15.2	0.74	0.78
D01	324	62.8	60.4	62.6	-2.4	-0.2	16.8	15.6	0.73	0.76
10-m Wind Speed (ms <sup>-1</sup> )										
Beijing	1	5.41	2.27	2.24	-3.14	-3.17	4.98	5.09	0.72	0.69
D03	30	5.73	3.26	3.20	-2.47	-2.53	4.60	4.65	0.62	0.61
D02	77	6.18	3.60	3.55	-2.58	-2.63	4.52	4.55	0.67	0.66
D01	324	5.67	3.38	3.36	-2.29	-2.31	4.29	4.30	0.60	0.61
10-m Wind Direction (°)										
Beijing	1	197.5	214.2	191.0	16.7	-6.6	73.9	73.9	0.79	0.80
D03	30	215.1	210.0	206.5	-6.9	-8.6	62.7	63.4	0.78	0.78
D02	77	214.4	212.2	208.9	-2.8	-5.5	65.4	65.4	0.76	0.76
D01	324	206.5	193.4	188.4	-13.1	-18.0	71.9	72.2	0.74	0.74

Hourly values are used for each station from 12 October to 19 November 2014. Where observation data are missing, model values were removed to ensure that sampling was consistent.

and performance is least good for the Beijing site where the bias is greater than 50% with both fields. However, the correlation coefficient at this site is slightly better than over the three model domains suggesting that the hourly variability in wind speeds is captured moderately well. If the underprediction of wind speeds extends above the surface, then this may lead to the build-up of gas-phase and aerosol species in the simulations and to overproduction of secondary aerosols due to unrealistic stagnation.

- 5 The model captures the 10 m wind direction reasonably well with both sets of data and the correlation coefficient is close to 0.80 for Beijing. It is notable that the correlation coefficient improves for most variables between domain 1 and domain 3, as the model resolution increases from 27 km to 3 km. Based on these comparisons with meteorological observations, and on subsequent comparison of pollutant concentrations, we find that the model performs marginally better using the ECMWF meteorological fields. With these fields the model captures the timing of pollution episodes better, leading to more realistic
- 10 pollutant behaviour, and we have therefore chosen ECMWF fields over FNL fields for our model studies.



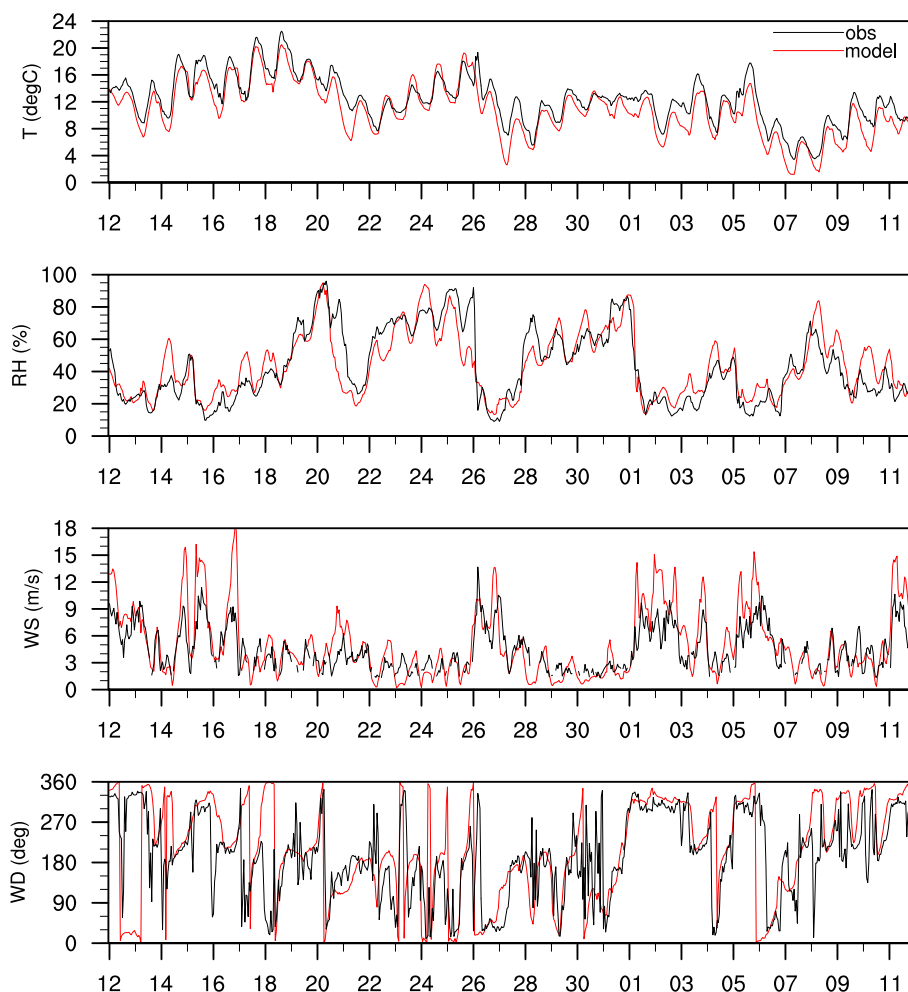


**Figure 2.** Comparison of meteorological measurements at 190–310 m on the IAP tower in Beijing with model simulations using ECMWF meteorological fields between 12 October and 12 November 2014.

Figure 2 presents an evaluation of meteorological variables with measurements from the IAP tower. We evaluate the model against measurements at 190–310 m (model level 4) to minimize the effects of buildings surrounding the site, which are not adequately resolved in the model. The daily maxima and minima in temperature are reproduced reasonably well with a small underestimation that averages less than 2 °C. The diurnal variations and averages for relative humidity, wind speed and wind direction are also captured well. The mean bias in relative humidity is 0.9% and the large underprediction at the airport meteorological station evident in Table 2 is not seen here, suggesting that it may be a surface level feature or reflect the overestimation of temperature at that location. Over the height of the tower (5 model levels) the diurnal variation in humidity drops by more than a factor of two, very similar to the reduction seen in the observations. The wind speed is slightly overestimated during windier periods, with a mean bias of 0.54 ms<sup>-1</sup>. Again, this suggests that the underestimation of 10-m wind speeds at mete-



orological stations seen in Table 2 is a surface feature in the model, and does not represent a systematic bias throughout the boundary layer. The synoptic patterns in all four variables are captured very well, highlighting the quality of the ECMWF meteorological data, and there is only one occasion on 20–21 October when substantial deviations in temperature and humidity are evident.

## 5 3.2 Air Quality

We ran the model for 41 days from 10 October to 19 November 2014 using ECMWF meteorology. The first 40 hours were set aside as model spin-up. A comparison of modelled pollutants against measurements from the CNEMC network is presented for October in Table 3 and the mean spatial distribution of  $PM_{2.5}$  during October is shown in Fig. 3. We do not include the November period here because emission controls were implemented across Beijing and surrounding provinces from the beginning of November. A full time-series of the comparison to observations is shown in Fig. 4

Table 3 shows a comparison of the key gas-phase and particulate species for all the surface pollutant stations from the observation network over the corresponding model domains. The model overpredicts average surface  $PM_{2.5}$  slightly (5–18%) across all domains. The correlation coefficient for hourly  $PM_{2.5}$  improves with resolution from 0.47 for domain 1 to 0.63 for domain 3 and 0.68 for the 12 Beijing sites. The model underestimates  $PM_{10}$  across all domains, although the biases are relatively small over Beijing. This underestimation may be attributed to neglect of mineral dust sources in the model, which play a relatively small role over Beijing at this time of year. CO is significantly underestimated for domain 1 but the biases reduce with increasing resolution and are smallest for the Beijing sites. The underestimation of CO for coarser domains may reflect the heterogeneity of sources, although the consistency of this bias and the relatively high levels of observed CO suggest an underestimate of CO sources across much of China in the emissions inventory. A similar effect is seen for  $NO_2$ , which is underestimated by 45% over the outer model domain, but by a much smaller margin over Northern China, and averages only 8% over the Beijing sites. While this may reflect an underestimate in emissions, the improvement is partly due to better representation of the emissions distribution for this shorter-lived pollutant on a finer grid.  $SO_2$  is underestimated by 13% over domain 1 but is overestimated over Beijing by a factor of three. This large overestimation for Beijing can be attributed to the recent rapid reduction in emissions in the region between 2010 and 2014 that are not represented in the 2010 inventory (Zheng et al., 2018). Ozone shows a contrasting trend, with an overestimate of 50% for domain 1 reducing to 5% for domain 3 and a 3% underestimation over Beijing. This may reflect the bias in  $NO_2$  concentrations, and is likely to be heavily influenced by the urban characteristics of most of the air quality stations.

For most pollutants, the correlation coefficient and slope improve substantially with resolution, and are better on a daily mean basis than at hourly resolution. This suggests that the day to day variability driven largely by regional meteorological processes is captured better than the diurnal variations driven by chemistry and local boundary layer mixing, as expected. This is particularly noticeable for ozone, although concentrations of this pollutant remain low at this time of year. Daily mean concentrations are typically used for most metrics of pollutant impacts on human health, and the reasonable model performance for daily averaged data suggests that it is suitable for assessment of these policy-relevant metrics.





**Table 3.** Comparison of pollutant concentrations with network measurements over the period 12–31 October 2014

	Number of Stations	Obs	Sim	Bias	RMSE hourly/daily	r hourly/daily	slope hourly/daily
PM <sub>2.5</sub> (µg m <sup>-3</sup> )							
Beijing stations	12	108.3	126.2	17.9	86.7/66.7	0.68/0.78	0.83/0.93
D03	137	92.6	109.3	16.7	72.2/52.2	0.63/0.74	0.71/0.80
D02	375	75.8	87.9	12.1	63.9/48.6	0.60/0.69	0.65/0.71
D01	1312	71.1	74.8	3.7	61.1/50.2	0.47/0.53	0.48/0.54
PM <sub>10</sub> (µg m <sup>-3</sup> )							
Beijing stations	12	155.4	141.5	-13.9	96.5/74.0	0.65/0.77	0.79/0.98
D03	137	165.7	122.9	-42.8	104.0/82.1	0.57/0.68	0.50/0.58
D02	375	138.0	98.6	-39.4	94.3/75.8	0.54/0.65	0.44/0.52
D01	1312	121.0	82.2	-38.8	89.0/76.7	0.42/0.47	0.32/0.37
CO (ppm)							
Beijing stations	12	1.11	0.94	-0.17	0.63/0.43	0.60/0.75	0.46/0.61
D03	137	1.17	0.83	-0.34	0.87/0.72	0.29/0.34	0.21/0.22
D02	375	1.14	0.66	-0.48	0.88/0.79	0.33/0.37	0.20/0.20
D01	1312	1.00	0.50	-0.50	0.79/0.73	0.32/0.34	0.13/0.14
NO <sub>2</sub> (ppb)							
Beijing stations	12	39.09	36.09	-3.00	19.33/11.10	0.62/0.80	0.66/0.83
D03	137	29.75	25.88	-3.87	18.95/14.32	0.47/0.54	0.45/0.51
D02	375	24.86	19.45	-5.41	16.99/13.21	0.49/0.55	0.44/0.50
D01	1312	22.73	12.45	-10.28	18.33/15.44	0.42/0.47	0.30/0.36
SO <sub>2</sub> (ppb)							
Beijing stations	12	3.92	12.27	8.35	11.88/10.55	0.27/0.52	0.68/1.74
D03	137	13.28	14.47	1.19	13.66/9.66	0.21/0.31	0.22/0.24
D02	375	12.23	13.21	0.98	13.19/9.01	0.24/0.34	0.26/0.28
D01	1312	10.27	8.93	-1.34	11.17/8.54	0.19/0.28	0.18/0.24
O <sub>3</sub> (ppb)							
Beijing stations	12	12.53	12.19	-0.34	13.92/6.49	0.47/0.67	0.44/0.82
D03	137	17.76	18.75	0.99	15.96/10.88	0.45/0.49	0.43/0.50
D02	375	21.23	23.08	1.85	17.19/12.80	0.42/0.43	0.37/0.40
D01	1312	21.44	32.29	10.85	22.44/17.03	0.29/0.27	0.27/0.25

The spatial distribution of mean PM<sub>2.5</sub> concentrations over 12–31 October is shown in Fig. 3. The distribution is captured reasonably well by the model, with the western parts of China showing clean air with concentrations less than 10 µg m<sup>-3</sup>)

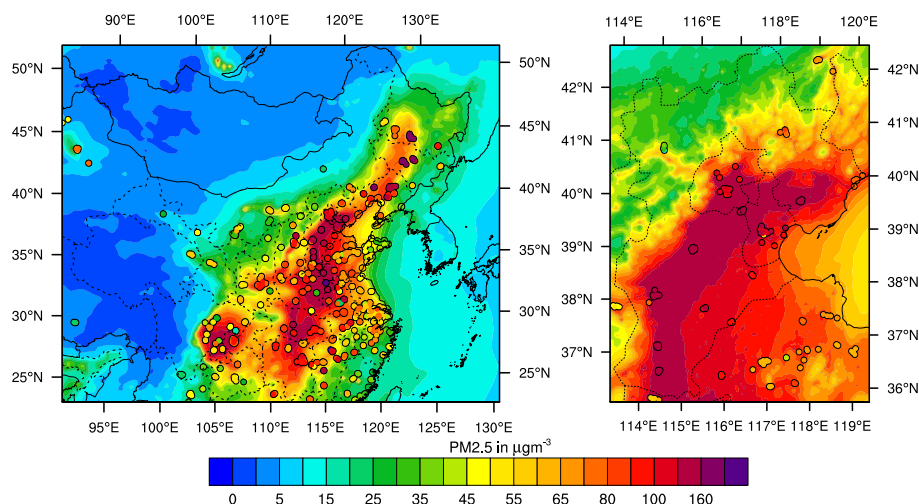


**Figure 3.** Average spatial distribution of  $\text{PM}_{2.5}$  over the period 12–31 October 2014 for model domain 1 (left) and domain 3 (right) along with observations shown in circles.

while the eastern, more populous parts of the country show average concentrations of  $70\text{--}150\ \mu\text{g m}^{-3}$ . Key hot-spots over the North China Plain, Central China and the Sichuan Basin are reproduced, and concentrations in coastal regions are notably lower, matching observations. The North China Plain is one of the most densely populated parts of the country, incorporating major cities such as Beijing, Tianjin, and Shijiazhuang, and frequently experiences heavy haze episodes with high levels of particulate matter (Wang et al., 2014; Gao et al., 2015a). Highest concentrations of  $\text{PM}_{2.5}$  occur on the western side of the North China Plain, where they are trapped by southeasterly winds against the Taihang mountains, and this is reproduced well by the model. There is a notable east-west gradient as concentrations drop off eastwards towards the coast. Over the mountains to the northwest of Beijing concentrations are much lower, typically less than  $40\ \mu\text{g m}^{-3}$ .

Figure 4 shows the time-series of key gas-phase and particulate pollutants averaged over the 12 network sites in Beijing. The general synoptic and diurnal patterns of  $\text{PM}_{2.5}$ ,  $\text{PM}_{10}$ , CO,  $\text{NO}_2$  and  $\text{O}_3$  are reproduced well by the model, including the magnitude of daily maxima and minima.  $\text{SO}_2$  is greatly overestimated in October, reflecting recent rapid emission reductions in Beijing (Zheng et al., 2018), and this is consistent with the findings of previous studies (Chen et al., 2016a; Gao et al., 2015a; Guo et al., 2016). However, we note that  $\text{SO}_2$  is reproduced much better from 15 November onwards, following the start of the heating season, highlighting the continuing major importance of this source. The observations show that the region experiences clear synoptic patterns of pollutant build-up over 4–5 days followed by sudden clean-out which is typically associated with frontal passage from the northwest (Guo et al., 2014). These synoptic patterns are seen more clearly for particulate matter than for gas-phase pollutants like  $\text{NO}_2$  and CO which exhibit a stronger diurnal signal reflecting chemical and dynamical processes. With the exception of  $\text{SO}_2$ , key pollutants and their variation over this period are reproduced well.

A more critical test of model performance is made by comparison of aerosol composition with measurements at IAP over this period, see Fig. 5. For all three episodes in October the model overestimates BC,  $\text{NO}_3$  and  $\text{NH}_4$  and underpredicts OC

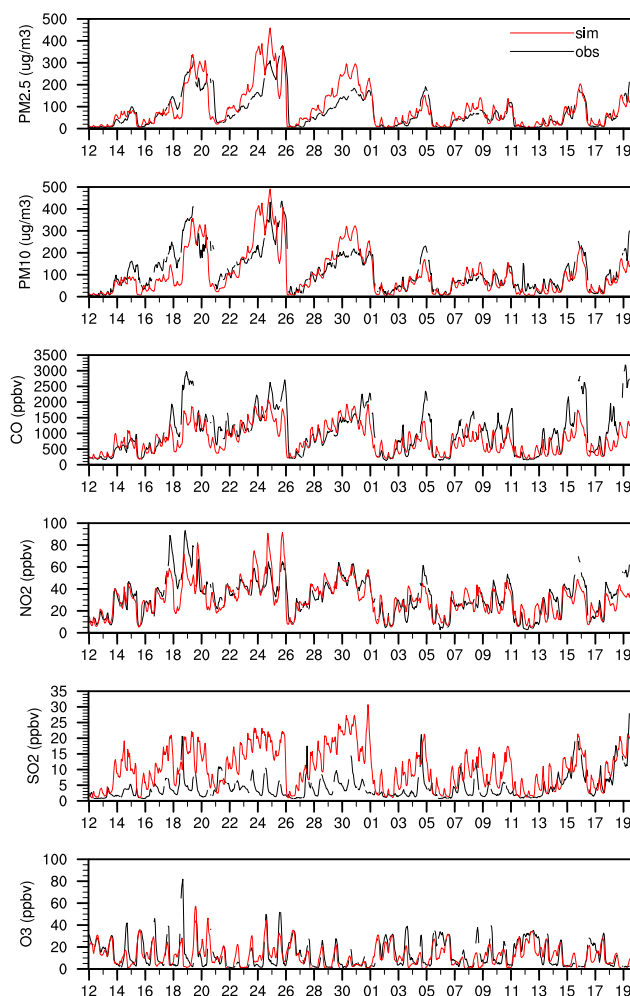


**Figure 4.** Mean time-series of surface pollutants over the 12 air quality stations in Beijing

and  $\text{SO}_4$ . The overestimation of BC likely reflects use of emissions for 2010, highlighting reductions between 2010 and 2014, but may also indicate insufficient removal in the model. The overprediction of  $\text{NO}_3$  and  $\text{NH}_4$  could be due to uncertainty in  $\text{NO}_2$  and  $\text{NH}_3$  emissions or to overestimated gas to particle conversion in the model. In particular, the model may overestimate secondary production of  $\text{NO}_3$  and  $\text{NH}_4$  during stagnant conditions such as those occurring during the three October episodes (note the low wind speeds shown in Fig. 2), but matches better during the first half of November, when conditions are less stagnant. The underestimation of  $\text{SO}_4$  occurs despite an overestimation of gas-phase  $\text{SO}_2$ , highlighting insufficient formation of  $\text{SO}_4$  in the model. The underestimation of OC can be explained by the absence of secondary organic aerosol in the chemical mechanism we have used.

The relative proportions of  $\text{SO}_4$  and  $\text{NH}_4$  to other components are similar at the surface and 260 m, while the proportion of OC is lower at 260 m and that of  $\text{NO}_3$  is higher. The model concentrations of  $\text{NO}_3$  and  $\text{SO}_4$  are 10–15% and 30% lower

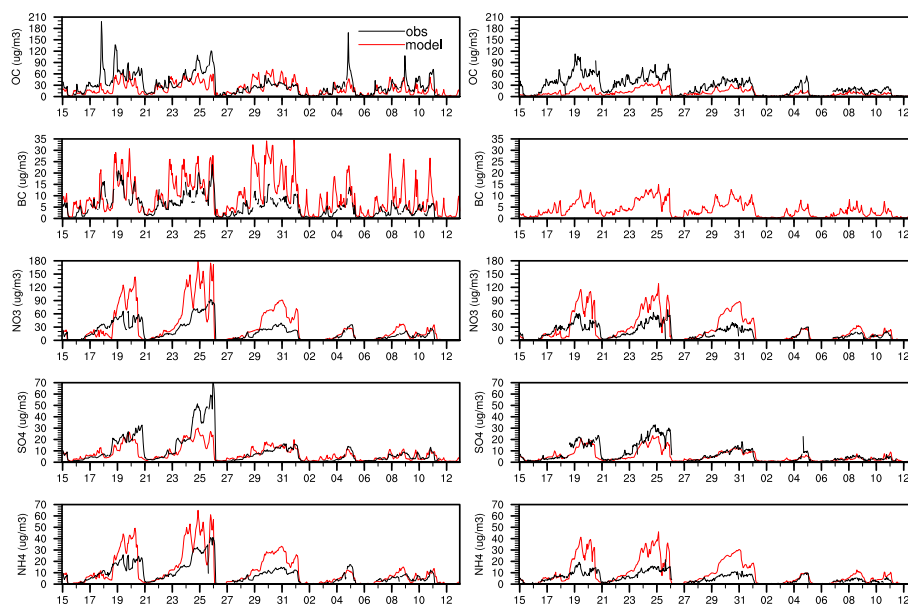


**Figure 5.** Measured and simulated aerosol components at the surface (left) and 260 m (right) on the IAP tower in Beijing

at 260 m, respectively, which is very similar to the observed reduction. The modelled  $\text{NH}_4$  is 22% lower at 260 m, less than the observed reduction of 33%, and this may be attributed to an overproduction of secondary  $\text{NH}_4$  in the model which reduces the vertical concentration gradient. Modelled OC falls off more quickly with altitude than in the observations (53% vs. 12%) and this is likely to be because the OC in the model is primary and therefore its vertical distribution reflects the surface source, while there is more secondary OC in the observations (Sun et al., 2016b) which leads to a weaker gradient with altitude.

#### 4 Investigating model sensitivity

While the baseline model simulation with ECMWF meteorological fields reproduces observed pollutant levels reasonably well, the comparisons have highlighted uncertainties associated with resolution, vertical mixing processes, and aerosol composition. We explore the sensitivity of our results to these factors here.

##### 10 4.1 Model resolution

Running the model at high resolution comes at a substantial cost in computing resources and simulation time. To investigate the gains that increased horizontal resolution provides, we sample all three model domains at the 12 Beijing stations and compare the results with observations. We use two-way nesting, so results from the nested domains feed back to the parent domain. To eliminate this effect, we perform an additional simulation over the parent domain only. Table 4 shows a comparison with measurements over Beijing in October for the different resolutions. In the nested simulation,  $\text{PM}_{2.5}$  is overestimated by 14% for domain 1, 19% for domain 2 and 16% for domain 3, but is underestimated by 8% for the domain 1 simulation without

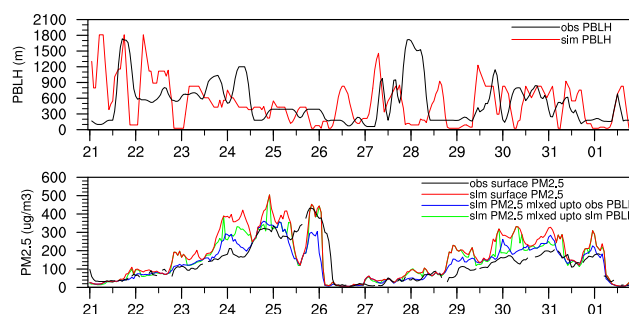


**Figure 6.** Simulated and observed boundary layer mixing height in metres (top) and simulated and observed  $\text{PM}_{2.5}$  in  $\mu\text{g m}^{-3}$  showing the effect of mixing up to the PBL height in the model (bottom) between 20 October and 2 November 2014.

nesting. Although the mean biases do not improve with higher resolution, reflecting the two-way nesting, there is a substantial improvement in the correlation coefficient (0.59 to 0.68) and slope (0.55 to 0.83) for  $\text{PM}_{2.5}$  when nesting is used, and this occurs for other pollutants too. For many variables the results sampled at 9-km resolution (D02) are slightly better than those sampled at 3-km resolution (D03), although it should be noted that results at D02 are influenced by the higher-resolution simulation at D03 through the two-way nesting. Results at 27-km resolution without nesting are substantially less good than those with two-way nesting, highlighting the important contribution of the coupling. We conclude that it is worth performing simulations at higher horizontal resolution as it gives a better representation of urban pollution levels.

## 4.2 Boundary layer mixing

Representing turbulent mixing processes in the boundary layer well is critical for simulating surface air quality. The nighttime boundary layer under stable meteorological conditions is particularly difficult to model, and we find that the mixing height is often severely underpredicted (and is as low as 20 m on several occasions) causing pollutant concentrations to reach unrealistically high levels. Nudging meteorological fields to ECMWF reanalysis data reduces this bias but does not remove it. After testing a number of different boundary layer algorithms we selected the Yonsei University (YSU) scheme (Hong et al., 2006) as it provides the best overall match to lidar-derived observations of boundary layer height. However, stable conditions remain a challenge for this scheme, and we therefore explore the sensitivity of simulated surface concentrations to boundary layer mixing under these conditions.

Figure 6 shows the time-series of simulated and observed planetary boundary layer (PBL) height. The observed PBL height was derived from lidar data at IAP using the cubic root gradient method of Yang et al. (2017). The simulated PBL height was diagnosed using the maximum decrease in the modelled  $\text{PM}_{2.5}$  profile to ensure a consistent definition. We compare the observed PBL height with the simulated height at IAP, and use  $\text{PM}_{2.5}$  measurements from the surface pollutant station at Aotizhongxin, the closest station to the IAP site (within 2 km) to assess the effect on  $\text{PM}_{2.5}$  concentrations. The PBL height shows highly variable behaviour over the day and from day to day. While the model average PBL height (514 m) is similar to the observed average height (509 m) over the haze episodes shown, the model severely underpredicts the nighttime PBL



**Table 4.** Impacts of model resolution on simulation of hourly pollutant concentrations in Beijing over 12–31 October 2014

	N points	Obs mean	Sim mean	Mean Bias	RMSE	r	slope
PM <sub>2.5</sub> (µg m <sup>-3</sup> )							
D03 (3-km)	3171	108.4	126.2	17.8	86.7	0.68	0.83
D02 (9-km)	3171	108.4	128.7	20.3	87.4	0.69	0.85
D01 (27-km)	3171	108.4	123.1	14.7	86.1	0.68	0.81
D01 (no nest)	3171	108.4	99.2	-9.2	83.2	0.59	0.55
PM <sub>10</sub> (µg m <sup>-3</sup> )							
D03	2670	155.4	141.5	-13.9	96.5	0.65	0.79
D02	2670	155.4	143.6	-11.8	96.6	0.65	0.80
D01	2670	155.4	137.9	-17.5	96.6	0.65	0.79
D01 (no nest)	2670	155.4	111.2	-44.2	99.8	0.58	0.54
CO (ppm)							
D03	3074	1.11	0.94	-0.17	0.63	0.60	0.46
D02	3074	1.11	0.95	-0.16	0.61	0.61	0.47
D01	3074	1.11	0.88	-0.23	0.61	0.64	0.44
D01 (no nest)	3074	1.11	0.68	-0.43	0.73	0.62	0.31
NO <sub>2</sub> (ppb)							
D03	3080	39.09	36.09	-3.00	19.33	0.62	0.66
D02	3080	39.09	35.55	-3.54	19.34	0.62	0.64
D01	3080	39.09	31.92	-7.17	18.33	0.67	0.62
D01 (no nest)	3080	39.09	21.81	-17.28	24.74	0.60	0.48
SO <sub>2</sub> (ppb)							
D03	3074	3.92	12.27	8.35	11.88	0.27	0.68
D02	3074	3.92	12.15	8.23	11.64	0.27	0.66
D01	3074	3.92	10.91	6.99	9.82	0.32	0.69
D01 (no nest)	3074	3.92	6.47	2.55	5.57	0.29	0.40
O <sub>3</sub> (ppb)							
D03	3046	12.56	12.19	-0.37	13.92	0.47	0.44
D02	3046	12.56	12.71	0.15	13.94	0.47	0.43
D01	3046	12.56	14.96	2.40	13.53	0.49	0.44
D01 (no nest)	3046	12.56	17.59	5.03	14.08	0.51	0.45

height on a number of occasions. Assuming that the PBL height reflects the efficiency of mixing in the boundary layer, we expect the model to overpredict surface pollutant concentrations under these stable nighttime conditions, and this is seen in the time-series of PM<sub>2.5</sub> at Aotizhongxin shown in Fig. 6. To account for misrepresentation of local boundary layer mixing,





we show the modelled  $\text{PM}_{2.5}$  vertically-averaged up to the simulated mixing height, to minimise the effect of underestimated mixing, and up to the observed mixing height, to provide a clearer comparison against  $\text{PM}_{2.5}$  observations. Mixing to the observed PBL height gives a substantial improvement in  $\text{PM}_{2.5}$  levels compared to observations, particularly for the episodes of 21–25 October and 27 October–1 November when the model significantly underestimates the PBL height. The simulated mean surface  $\text{PM}_{2.5}$  concentration during the period is reduced from 169 to  $130 \mu\text{g m}^{-3}$  (the observed mean is  $129 \mu\text{g m}^{-3}$ ) and the RMSE is reduced from 94 to  $65 \mu\text{g m}^{-3}$ .

These results highlight that accurate reproduction of surface pollutant levels with the model is tightly linked to how well it can reproduce PBL mixing. We note that the PBL shows a steady decline in height over the pollution episode during 21–25 October, and  $\text{PM}_{2.5}$  shows a consistent build-up over the same period. This provides some observational evidence for the radiative feedback between aerosol concentrations and mixing height, and this appears to be captured relatively well by the model, as shown in previous studies (Gao et al., 2015b). To further improve simulation of surface pollutant concentrations, additional research is needed to accurately model PBL mixing processes in urban environments. Profiles of aerosol and meteorological variables from high-resolution lidar measurements provide an important aid to such investigations.

### 4.3 Regional $\text{NH}_3$ emissions

The aerosol components  $\text{NO}_3$  and  $\text{NH}_4$  are overestimated in these simulations, as shown in Fig. 5. These components are governed by secondary production from their gaseous precursors  $\text{NO}_2$  and  $\text{NH}_3$ . Since the concentration of  $\text{NO}_2$  is close to that observed, we perform a short sensitivity study over the pollution episode from 21–25 October with  $\text{NH}_3$  emissions over the North China Plain reduced by 50% to investigate the effect on aerosol composition. We find that the reduction in  $\text{NH}_3$  emissions not only reduces  $\text{NH}_4$  concentrations but also  $\text{NO}_3$  and, to a lesser degree,  $\text{SO}_4$  concentrations, see Fig. 7. This is likely to be because  $\text{NH}_3$  is the limiting reactant in the formation of  $\text{NH}_4\text{NO}_3$  that directly controls the concentration of both  $\text{NH}_4$  and  $\text{NO}_3$  aerosols (Gao et al., 2016b) and consequently a reduction in  $\text{NH}_4\text{NO}_3$  may suppress the secondary formation of  $\text{SO}_4$  due to reduced aerosol surface area on which it can form. These reductions in aerosol components reduce total  $\text{PM}_{2.5}$  concentration by approximately 26% bringing it closer to observed concentrations at the IAP site, see Table 5. Ammonia emissions were reported to be 1574 kt/yr over the Beijing-Tianjin-Hebei region in 2010 (Zhou et al., 2015) while those in the MEIC emissions inventory used here are only 540 kt/yr. Given that our  $\text{NH}_3$  emissions are already low compared with other studies (Kang et al., 2016), we do not reduce them further in this study. However, we demonstrate that  $\text{PM}_{2.5}$  concentrations during this period are highly sensitive to  $\text{NH}_3$  emissions, consistent with the findings of other studies (Zhang et al., 2016), and highlight this issue for further investigation.

## 5 APEC Emission Controls

The Asia-Pacific Economic Cooperation (APEC) summit was held from 10–12 November 2014 in Beijing, and was the focus of short-term emission controls to ensure good air quality over the period. Emission controls were applied in Beijing and surrounding regions including Tianjin city, the provinces of Hebei, Shanxi and Shandong, and Inner Mongolia Autonomous

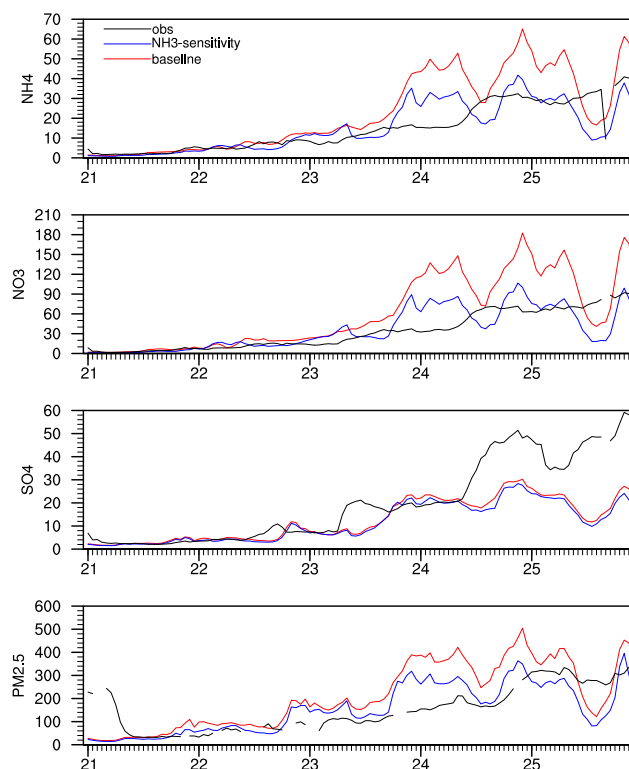


**Figure 7.** Time-series of aerosol components  $\text{NH}_4$ ,  $\text{NO}_3$  and  $\text{SO}_4$  at the IAP site and  $\text{PM}_{2.5}$  at Aotizhongxin showing simulated concentrations (in  $\mu\text{g m}^{-3}$ ) from the baseline model run and reduced  $\text{NH}_3$  emissions run compared to observations.

**Table 5.** Mean concentrations (in  $\mu\text{g m}^{-3}$ ) at IAP during 21–25 October 2014

Species	Control run	Reduced $\text{NH}_3$ run	Observations
$\text{PM}_{2.5}$	210.8	154.9	157.5
$\text{NO}_3$	61.28	36.60	33.81
$\text{NH}_4$	23.11	15.24	15.03
$\text{SO}_4$	12.70	11.59	20.40

Region. More than 460 businesses with high emissions in Beijing were required to limit or stop their production during 3–12 November 2014 (Tang et al., 2015; Wang et al., 2016a; Guo et al., 2016). The number of private vehicles in operation over this period was reduced by about 50% through odd/even license-plate restrictions. Further, 9300 enterprises were suspended, 3900 enterprises were ordered to limit production, and more than 40,000 construction sites were shut down across the North China region (Wang et al., 2016b; Tang et al., 2015). The start-up of municipal winter heating systems was delayed until

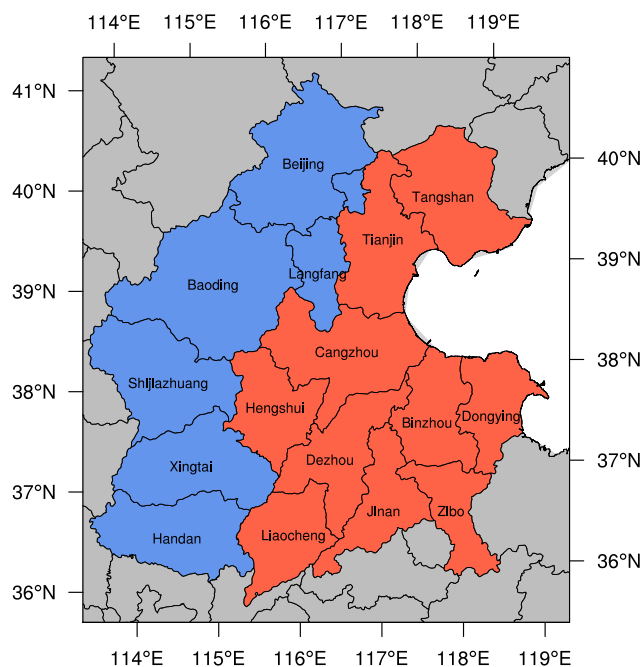


**Figure 8.** Map showing districts where major emissions controls were implemented during the APEC period. During phase 1 emissions were restricted in Beijing and western Hebei (blue) and in phase 2 controls were additionally applied over other parts of the North China Plain (red).

**Table 6.** Emission controls during APEC period

Emission sector	Emission reduction (%)	
	Beijing	Other Districts
Industry	50	35
Power	50	35
Agriculture	40	30
Residential	40	30
Transport	40	30
PM coarse (all sectors)	80	–

APEC1: Beijing, Langfang, Baoding, Shijiazhuang, Xingtai, Handan  
 APEC2: APEC1 + Tangshan, Tianjin, Cangzhou, Hengshui, Dezhou, Binzhou, Dongying, Zibo, Jinan and Liaocheng

15 November, after the summit. Implementation of these emission controls resulted in significant impacts on regional pollutant transport and local pollutant contributions (Meng et al., 2014; Sun et al., 2016b; Gao et al., 2017).

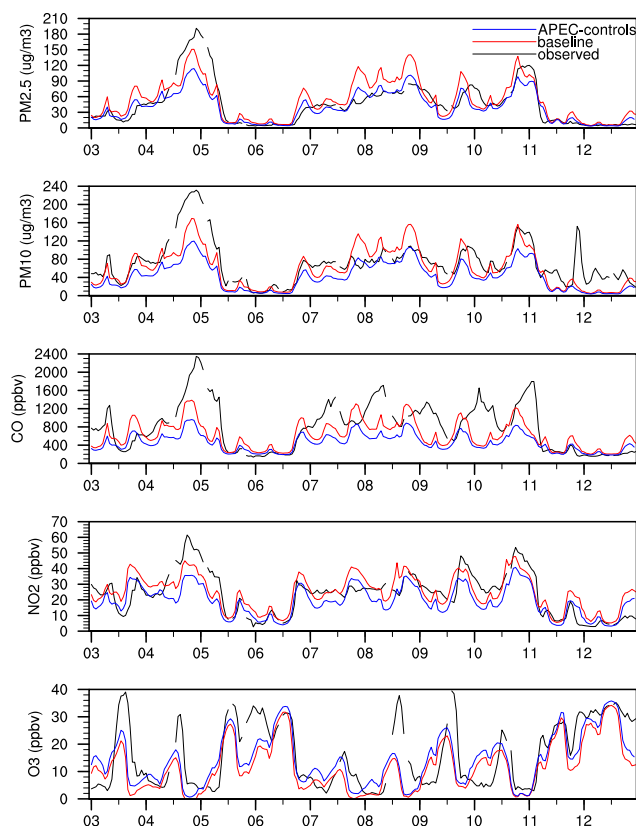


**Figure 9.** Time-series of surface pollutants averaged over the 12 measurement stations in Beijing during the APEC period.

Previous model studies of the APEC period have adopted different estimates of the emission reductions imposed (Guo et al., 2016; Gao et al., 2017; Wen et al., 2016; Liu et al., 2017; Wang et al., 2017). The most detailed study of emission reductions considered application of controls in two distinct phases (Wen et al., 2016), and we have chosen to implement these controls in our study, as the emission reductions applied are consistent with observation-based assessments of regional emission controls (Li et al., 2017b). During the initial phase (APEC1, 3–5 November), emission controls were implemented in Beijing and the western side of the North China Plain. In a subsequent phase (APEC2, 6–12 November) controls were applied over a wider region including eastern Hebei and parts of Shandong. We represent these controls in the model over the districts shown in Fig. 8, following Li et al. (2017b), and neglect smaller changes in emissions in other districts and more distant provinces. Controls were applied across different activity sectors following Wen et al. (2016) and Li et al. (2017b), see Table 6.

Figure 9 shows the effect of these controls on key pollutants over the period 3–12 November. There is a minor pollution episode over 4–5 November, and the model underestimates  $\text{PM}_{2.5}$  levels over this period in the baseline run even without the emission controls. This may reflect an underestimation of OC as the simulation of secondary inorganic aerosol for these two days is relatively good (see Fig. 5).  $\text{PM}_{2.5}$  levels are very well matched in the period 6–9 November leading up to the summit when applying the emission controls.  $\text{PM}_{10}$  levels are underestimated in the simulations, but this is strongly influenced

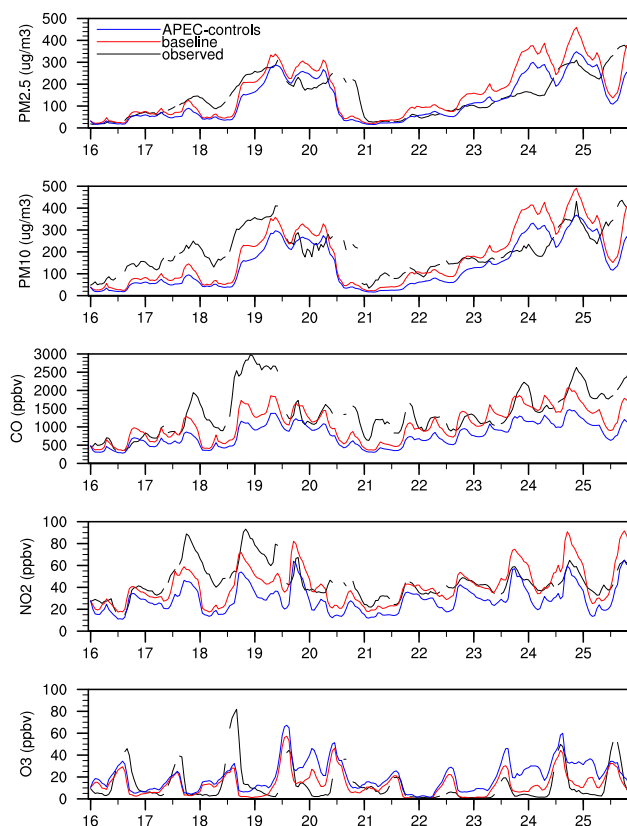


**Figure 10.** Time-series of surface pollutants averaged over the 12 measurement stations in Beijing during 16–25 October 2014.

by what may be a minor dust episode on 11–12 November, when coarse particles were high but  $\text{PM}_{2.5}$  remained very low. Overall, the controls had a notable effect, reducing concentrations by 20–30% for all pollutants except  $\text{O}_3$ , which showed a small increase as expected for lower levels of NO. Over the critical 10–12 November meeting period,  $\text{PM}_{2.5}$ ,  $\text{PM}_{10}$ , CO and  $\text{NO}_2$  were reduced by 21%, 26%, 22% and 22% respectively, see Table 7. The reduction in  $\text{PM}_{2.5}$  is very similar to the 22% found in previous studies (Gao et al., 2017). However, the absolute improvement in air quality over the meeting period was small, averaging less than  $10 \mu\text{g m}^{-3}$  for  $\text{PM}_{2.5}$ , reflecting the relatively clean conditions over the period. Average  $\text{PM}_{2.5}$  in the baseline simulation was  $39 \mu\text{g m}^{-3}$ , close to the observed  $36 \mu\text{g m}^{-3}$ . Under these conditions the key air quality standard, a 24-hour averaged  $\text{PM}_{2.5}$  of  $75 \mu\text{g m}^{-3}$ , corresponding to a Chinese Air Quality Index (AQI) of 100, would have been met in the model simulation even without the controls.

- 10 To explore the importance of meteorological conditions in contributing to the favourable air quality during the APEC period, we apply the same magnitude, location and duration of emission controls to the major pollution episode at the end of October. Fig 10 shows the effect of these controls on key pollutants over 16–25 October. The controls reduced pollutant concentrations by a larger amount than during the APEC period, but the relative improvements of 23–38% were very similar. The absolute pollutant concentrations were much higher than in November. This can be attributed to lower wind speeds and to winds



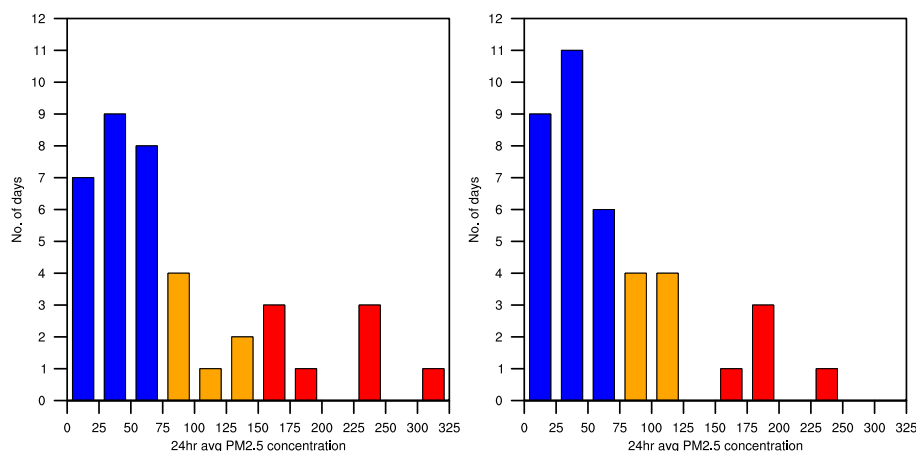
from the South and East bringing air from across the North China Plain, in contrast to the APEC period which experienced higher wind speeds and air from the clean northwest sector. The 3-day baseline average concentrations over 23–25 October for  $\text{PM}_{2.5}$ ,  $\text{PM}_{10}$ , CO and  $\text{NO}_2$  were  $279 \mu\text{g m}^{-3}$ ,  $310 \mu\text{g m}^{-3}$ , 1.48 ppm and 53 ppb respectively, substantially exceeding air quality standards. The difference in baseline  $\text{PM}_{2.5}$  concentrations between the October and November periods without emission controls, 279 vs.  $39 \mu\text{g m}^{-3}$ , highlights the dominant role played by meteorology in bringing clean air during APEC. The emission controls have a much larger absolute effect during the October episode than in the APEC period, with reductions in  $\text{PM}_{2.5}$  of  $65 \mu\text{g m}^{-3}$  for 23–25 October, bringing average  $\text{PM}_{2.5}$  levels down to  $214 \mu\text{g m}^{-3}$ . However, this is insufficient to meet the standards needed for clean air of  $75 \mu\text{g m}^{-3}$ . This indicates that the emission control policies applied would have failed to produce the desired results if the meeting had been held at the end of October.

Table 8 presents the effect on aerosol components and gas-phase pollutants at the IAP tower. During the emission controls in both the polluted October and cleaner November periods, primary components were reduced by 31–34% while secondary components were reduced by only 3–18%. This suggests that pollution episodes dominated by primary aerosols may be more easily controlled. This has serious implications for winter haze episodes over the North China Plain because much of the increase in aerosol loading is contributed by regional secondary aerosols (see Sun et al., 2016b).

To investigate the feasibility of meeting air quality standards during pollution episodes such as that on 21–25 October, we ran the model with all anthropogenic emissions removed over the North China Plain region shown in Fig. 8 from 16–25 October. The 3-day average concentrations over 23–25 October showed substantial reductions: 83% for  $\text{PM}_{2.5}$ , 82% for  $\text{PM}_{10}$ , 79% for CO, 99% for  $\text{NO}_2$  and 88% for  $\text{SO}_2$ . Average  $\text{PM}_{2.5}$  concentrations were reduced from  $279 \mu\text{g m}^{-3}$  to  $48 \mu\text{g m}^{-3}$ , demonstrating that air quality standards can be met on highly polluted days, at least in theory, under the most stringent emission controls. From this simulation, and accounting for nonlinearity in secondary aerosol formation, we estimate that a 92% emission reduction over the 10 day period would have been needed to keep the average concentrations for 23–25th October below  $75 \mu\text{g m}^{-3}$ . Even accounting for the model overestimation of average  $\text{PM}_{2.5}$  during this period, driven principally by a high bias on 24 October, we find that an 85% emission reduction would be required, substantially more than is feasible realistically. It is clear from this analysis that emissions controls would need to be applied over a much wider area over neighbouring provinces if the air quality standards in Beijing were to be met.

Finally, we analyse the full simulation period (12 October–19 November) to investigate how many days would meet the "blue-sky" criteria of 24-hour average  $\text{PM}_{2.5}$  concentrations less than  $75 \mu\text{g m}^{-3}$  with and without the controls that were applied. To remove any model bias we use the relative benefits of controls derived from the model simulations and apply these reductions to the daily observed  $\text{PM}_{2.5}$  levels averaged over the 12 air quality stations in Beijing to generate a scenario representing the effect of emission controls. For 3–12 November, when emission controls were actually in place, we use the observed  $\text{PM}_{2.5}$  concentrations unaltered. We assume a reduction in  $\text{PM}_{2.5}$  of 22% at other times, representing an average of the responses seen over the October and November periods discussed above. To evaluate the effect of differences between modelled and observed aerosol composition on this scaling, given that primary aerosols are reduced more efficiently than secondary aerosols (Table 8), we apply the modelled reductions for each component to the observed component concentrations to find the total reduction in PM. This is found to be 22% for both October and November periods, suggesting that this scaling





**Figure 11.** Frequency distribution of daily average  $\text{PM}_{2.5}$  over 12 October–19 November 2014 showing the number of days meeting thresholds of  $75 \mu\text{g m}^{-3}$  (blue) and  $150 \mu\text{g m}^{-3}$  (blue plus orange) without (left panel) and with (right panel) emission controls.

is appropriate and robust to uncertainties in model aerosol composition. For the scenario with no controls, we apply an increase based on the November run of 16–33% for 3–12 November to estimate what the observations would have been, and use the observations on other days unaltered. With these scenarios we find that 15 of the 39 days considered failed to meet the blue-sky criteria of daily average  $\text{PM}_{2.5}$  concentrations less than  $75 \mu\text{g m}^{-3}$  without controls, and this fell to 13 days when the controls were implemented, a modest decrease of 2 days, see Fig. 11. However, if we choose a higher threshold of  $150 \mu\text{g m}^{-3}$  (AQI of 200), the emission controls appear more effective, reducing the number of exceedances from 8 days to 5 days, and with a threshold of  $200 \mu\text{g m}^{-3}$  (AQI of 250) the number of exceedances falls from 4 days to 1 day.

To organize a three-day meeting such as APEC successfully, all three days must individually meet the chosen air quality criteria. We find that without emission controls, only 9 out of 37 possible three-day time slots in our simulation period meet the criteria, including only 3 out of the 8 available during the APEC period of 3–12 November. Under the emission controls, the meeting could have been organized on 14 out of the 37 slots, including all 8 during early November. This suggests that the emission controls were only sufficient to provide an additional 5 time slots to hold a three-day event meeting the criteria. Interestingly, these all occur during the APEC period, highlighting that while favourable weather conditions were vital for meeting the air quality criteria, the emission controls provided critical support in achieving the  $75 \mu\text{g m}^{-3}$  threshold needed to realise blue sky conditions. Specifically, in the absence of emission controls the first day of the APEC meeting (10 November) would have exceeded the air-quality standards. In this respect, it is reasonable to claim that the APEC emission controls were a success. However, it is clear that favourable meteorology was essential in making it possible for the emission controls to produce the marginal improvements needed to meet the air quality standards.

It should be noted that 23 out of the 37 possible three-day time periods, more than 60%, would not have met the standards even under the emission controls applied. It is therefore clear that much more stringent controls are needed in future to counter the effect of unfavourable meteorological conditions. While greater reductions in the magnitude of emissions are required, it



**Table 7.** Influence of emission controls averaged over Beijing air quality stations in October and November

Species	Observed		Model	
	Mean	Baseline	Controls	Improvement
APEC period (10–12 November)				
PM <sub>2.5</sub> ( $\mu\text{g m}^{-3}$ )	36.1	39.3	31.1	8.2 (20.9%)
PM <sub>10</sub> ( $\mu\text{g m}^{-3}$ )	65.3	43.9	32.5	11.4 (26.0%)
CO (ppm)	0.64	0.48	0.38	0.11 (22.0%)
NO <sub>2</sub> (ppb)	19.0	20.6	16.0	4.6 (22.3%)
SO <sub>2</sub> (ppb)	2.1	6.1	4.2	1.9 (30.8%)
O <sub>3</sub> (ppb)	20.0	16.5	19.0	-2.5 (-15.3%)
October period (23–25 October)				
PM <sub>2.5</sub> ( $\mu\text{g m}^{-3}$ )	216.1	278.8	213.7	65.1 (23.3%)
PM <sub>10</sub> ( $\mu\text{g m}^{-3}$ )	263.8	309.6	236.4	73.2 (23.6%)
CO (ppm)	1.77	1.48	1.05	0.44 (29.6%)
NO <sub>2</sub> (ppb)	46.3	53.2	34.9	18.3 (34.4%)
SO <sub>2</sub> (ppb)	4.0	18.6	11.6	7.0 (37.7%)
O <sub>3</sub> (ppb)	11.4	15.2	26.7	-11.5 (-75.5%)

is important that these are applied over a much larger area, including in the neighbouring provinces that surround the North China Plain.

## 6 Conclusions

We have demonstrated that using a high-resolution nested air quality model we can reproduce the observed hourly variation of major pollutants in Beijing during October–November 2014 reasonably well. We capture the synoptic drivers of air quality well, including the build-up of pollutants during pollution episodes and the subsequent cleaning effect of winds from the northwest. The concentrations of PM<sub>2.5</sub>, the dominant pollutant in this season, are reproduced well, and we show that where the model is biased high, typically during nighttime, underlying weaknesses in the treatment of turbulent mixing in the planetary boundary layer are often responsible. We show that use of two-way nesting to high resolution brings a substantial benefit in reproducing observed pollutant concentrations, even when comparing at the coarsest resolution used. Thorough evaluation against aerosol composition measurements over the period highlight some weaknesses in representation of key aerosol components, particularly the balance between SO<sub>4</sub>, NO<sub>3</sub> and NH<sub>3</sub> which requires more detailed analysis.

We show that short-term emission controls played a valuable role in improving air quality over the APEC period, but that their overall contribution was relatively small, with average reductions of 20–26% for key pollutants. Without the controls, average PM<sub>2.5</sub> levels are likely to have exceeded the national standard of 75  $\mu\text{g m}^{-3}$  on 10 November, the first day of the APEC



**Table 8.** Influence of emission controls at the IAP site in October and November

Species	Observed		Model	
	Mean	Baseline	Controls	Improvement
APEC period (10–12 November)				
OC ( $\mu\text{g m}^{-3}$ )	30.6	9.8	6.8	3.06 (31.1%)
BC ( $\mu\text{g m}^{-3}$ )	3.4	4.8	3.2	1.63 (33.8%)
NO <sub>3</sub> ( $\mu\text{g m}^{-3}$ )	10.9	8.6	8.3	0.27 (3.2%)
NH <sub>4</sub> ( $\mu\text{g m}^{-3}$ )	5.0	3.8	3.5	0.30 (8.0%)
SO <sub>4</sub> ( $\mu\text{g m}^{-3}$ )	4.8	3.5	2.9	0.60 (17.0%)
CO (ppm)	2.60	0.68	0.52	0.16 (24.0%)
NO <sub>2</sub> (ppb)	17.2	30.2	22.9	7.36 (24.3%)
SO <sub>2</sub> (ppb)	10.4	9.4	6.3	3.07 (32.8%)
O <sub>3</sub> (ppb)	3.5	17.6	21.6	-4.04 (-23.0%)
October period (23–25 October)				
OC ( $\mu\text{g m}^{-3}$ )	60.5	39.5	26.7	12.79 (32.4%)
BC ( $\mu\text{g m}^{-3}$ )	10.2	16.5	11.0	5.49 (33.2%)
NO <sub>3</sub> ( $\mu\text{g m}^{-3}$ )	51.3	95.0	79.7	15.32 (16.1%)
NH <sub>4</sub> ( $\mu\text{g m}^{-3}$ )	21.1	35.2	29.9	5.40 (15.3%)
SO <sub>4</sub> ( $\mu\text{g m}^{-3}$ )	31.2	18.4	15.8	2.53 (13.8%)
CO (ppm)	2.92	2.03	1.43	0.60 (29.5%)
NO <sub>2</sub> (ppb)	44.2	78.1	57.8	20.30 (26.0%)
SO <sub>2</sub> (ppb)	18.4	26.5	16.5	9.93 (37.5%)
O <sub>3</sub> (ppb)	5.9	10.3	22.1	-11.8 (-114.7%)

meeting, but the effects were largely incremental, highlighting the important role played by favourable meteorology during the period. If the APEC meeting had been held at a different time, particularly at the end of October, air quality standards would not have been achieved with the emission controls applied. We find that the relative effect of the controls during the pollution episodes of late October are very similar to those during the clean APEC period, averaging 23% for PM<sub>2.5</sub>. Much greater  
 5 emission reductions of at least 85% would have been needed over the North China Plain region to bring pollutant levels down to meet air quality standards. It is clear that under the stable meteorological conditions present during these pollution episodes much more stringent emission controls are needed than those that were applied, and that these need to be implemented over a much wider region of Northern China. Our study demonstrates the value of short-term emission controls, but highlights that long-term, sustained emission reductions on a regional scale are required to bring blue skies to Beijing.



*Code and data availability.* The WRF-Chem code is available from <http://www2.mmm.ucar.edu/wrf/users/download/>. The namelist for the model and surface pollutant distributions generated in this study will be made available from the Lancaster University data archive at <http://dx.doi.org/10.15125/XXXXXX>.

*Author contributions.* TA, OW and ZW designed this study, and TA performed the model simulations and analysis. JL provided emissions data and expertise on the model set-up, TY provided the lidar data and guidance on deriving PBL height, and YS, WX and ZW provided measurement data from the IAP tower. TA and OW prepared the manuscript with input from all coauthors.

*Competing interests.* The authors declare that they have no conflict of interest

*Acknowledgements.* OW thanks the UK Natural Environment Research Council for support under grants NE/N006925/1 and NE/N006976/1. YS thanks the National Natural Science Foundation of China (Grant No. 91744207).



## References

- Batterman, S., Xu, L., Chen, F., Chen, F., and Zhong, X.: Characteristics of PM<sub>2.5</sub> concentrations across Beijing during 2013–2015, *Atmospheric Environment*, 145, 104–114, <https://doi.org/10.1016/j.atmosenv.2016.08.060>, 2016.
- Bieser, J., Aulinger, A., Matthias, V., Quante, M., and Denier Van Der Gon, H. A. C.: Vertical emission profiles for Europe based on plume  
5 rise calculations, *Environmental Pollution*, 159, 2935–2946, <https://doi.org/10.1016/j.envpol.2011.04.030>, 2011.
- Chen, D., Liu, Z., Fast, J., and Ban, J.: Simulations of sulfate-nitrate-ammonium (SNA) aerosols during the extreme haze events over northern  
China in October 2014, *Atmospheric Chemistry and Physics*, 16, 10 707–10 724, <https://doi.org/10.5194/acp-16-10707-2016>, 2016a.
- Chen, F. and Dudhia, J.: Coupling an Advanced Land Surface–Hydrology Model with the Penn State–NCAR MM5 Mod-  
eling System. Part II: Preliminary Model Validation, *Monthly Weather Review*, 129, 587–604, [https://doi.org/10.1175/1520-0493\(2001\)129<0587:CAALSH>2.0.CO;2](https://doi.org/10.1175/1520-<br/>10 0493(2001)129<0587:CAALSH>2.0.CO;2), 2001.
- Chen, H., Li, J., Ge, B., Yang, W., Wang, Z., Huang, S., Wang, Y., Yan, P., Li, J., and Zhu, L.: Modeling study of source contributions and  
emergency control effects during a severe haze episode over the Beijing–Tianjin–Hebei area, *Science China Chemistry*, 58, 1403–1415,  
<https://doi.org/10.1007/s11426-015-5458-y>, 2015a.
- Chen, W., Tang, H., and Zhao, H.: Diurnal, weekly and monthly spatial variations of air pollutants and air quality of Beijing, *Atmospheric  
15 Environment*, 119, 21–34, <https://doi.org/10.1016/j.atmosenv.2015.08.040>, 2015b.
- Chen, Z., Xu, B., Cai, J., and Gao, B.: Understanding temporal patterns and characteristics of air quality in Beijing: A local and regional  
perspective, *Atmospheric Environment*, 127, 303–315, <https://doi.org/10.1016/j.atmosenv.2015.12.011>, 2016b.
- Clough, S. A., Shephard, M. W., Mlawer, E. J., Delamere, J. S., Iacono, M. J., Cady-Pereira, K., Boukabara, S., and Brown, P. D.: Atmospheric  
radiative transfer modeling: A summary of the AER codes, *Journal of Quantitative Spectroscopy and Radiative Transfer*, 91, 233–244,  
20 <https://doi.org/10.1016/j.jqsrt.2004.05.058>, 2005.
- Emmons, L. K., Walters, S., Hess, P. G., Lamarque, J.-F., Pfister, G. G., Fillmore, D., Granier, C., Guenther, A., Kinnison, D., Laepple, T.,  
Orlando, J., Tie, X., Tyndall, G., Wiedinmyer, C., Baughcum, S. L., and Kloster, S.: Description and evaluation of the Model for Ozone and  
Related chemical Tracers, version 4 (MOZART-4), *Geoscientific Model Development*, 3, 43–67, <https://doi.org/10.5194/gmd-3-43-2010>,  
2010.
- 25 Fast, J. D., Gustafson, W. I., Easter, R. C., Zaveri, R. A., Barnard, J. C., Chapman, E. G., Grell, G. A., and Peckham, S. E.: Evolution of  
ozone, particulates, and aerosol direct radiative forcing in the vicinity of Houston using a fully coupled meteorology–chemistry–aerosol  
model, *Journal of Geophysical Research Atmospheres*, 111, 1–29, <https://doi.org/10.1029/2005JD006721>, 2006.
- Gao, J., Peng, X., Chen, G., Xu, J., Shi, G.-L., Zhang, Y.-C., and Feng, Y.-C.: Insights into the chemical characterization and sources of PM<sub>2.5</sub>  
in Beijing at a 1-h time resolution, *Science of The Total Environment*, 542, 162–171, <https://doi.org/10.1016/j.scitotenv.2015.10.082>,  
30 2016a.
- Gao, M., Carmichael, G. R., Wang, Y., Saide, P. E., Yu, M., Xin, J., Liu, Z., and Wang, Z.: Modeling study of the 2010 regional haze event  
in the North China Plain, *Atmospheric Chemistry and Physics*, 15, 22 781–22 822, <https://doi.org/doi:10.5194/acp-16-1673-2016>, 2015a.
- Gao, M., Carmichael, G. R., Saide, P. E., Lu, Z., Yu, M., Streets, D. G., and Wang, Z.: Response of winter fine particulate mat-  
ter concentrations to emission and meteorology changes in North China, *Atmospheric Chemistry and Physics*, 16, 11 837–11 851,  
35 <https://doi.org/10.5194/acp-16-11837-2016>, 2016b.



- Gao, M., Liu, Z., Wang, Y., Lu, X., Ji, D., Wang, L., Li, M., Wang, Z., Zhang, Q., and Carmichael, G. R.: Distinguishing the roles of meteorology, emission control measures, regional transport, and co-benefits of reduced aerosol feedbacks in "APEC Blue", *Atmospheric Environment*, 167, 476–486, <https://doi.org/10.1016/j.atmosenv.2017.08.054>, 2017.
- Gao, Y., Liu, X., Zhao, C., and Zhang, M.: Emission controls versus meteorological conditions in determining aerosol concentrations in Beijing during the 2008 Olympic Games, *Atmospheric Chemistry and Physics*, 11, 12 437–12 451, <https://doi.org/10.5194/acp-11-12437-2011>, 2011.
- Gao, Y., Zhang, M., Liu, Z., Wang, L., Wang, P., Xia, X., Tao, M., and Zhu, L.: Modeling the feedback between aerosol and meteorological variables in the atmospheric boundary layer during a severe fog-haze event over the North China Plain, *Atmospheric Chemistry and Physics*, 15, 4279–4295, <https://doi.org/10.5194/acp-15-4279-2015>, 2015b.
- 10 Grell, G. a., Peckham, S. E., Schmitz, R., McKeen, S. a., Frost, G., Skamarock, W. C., and Eder, B.: Fully coupled "online" chemistry within the WRF model, *Atmospheric Environment*, 39, 6957–6975, <https://doi.org/10.1016/j.atmosenv.2005.04.027>, 2005.
- Guenther, A. B., Jiang, X., Heald, C. L., Sakulyanontvittaya, T., Duhl, T., Emmons, L. K., and Wang, X.: The model of emissions of gases and aerosols from nature version 2.1 (MEGAN2.1): An extended and updated framework for modeling biogenic emissions, *Geoscientific Model Development*, 5, 1471–1492, <https://doi.org/10.5194/gmd-5-1471-2012>, 2012.
- 15 Guo, J., He, J., Liu, H., Miao, Y., Liu, H., and Zhai, P.: Impact of various emission control schemes on air quality using WRF-Chem during APEC China 2014, *Atmospheric Environment*, 140, 311–319, <https://doi.org/10.1016/j.atmosenv.2016.05.046>, 2016.
- Guo, S., Hu, M., Zamora, M. L., Peng, J., Shang, D., Zheng, J., Du, Z., Wu, Z., Shao, M., Zeng, L., Molina, M. J., and Zhang, R.: Elucidating severe urban haze formation in China, *Proceedings of the National Academy of Sciences*, 111, 17 373–17 378, <https://doi.org/10.1073/pnas.1419604111>, 2014.
- 20 Hong, S.-Y., Noh, Y., and Dudhia, J.: A New Vertical Diffusion Package with an Explicit Treatment of Entrainment Processes, *Monthly Weather Review*, 134, 2318–2341, <https://doi.org/10.1175/MWR3199.1>, 2006.
- Kajino, M., Ueda, H., Han, Z., Kudo, R., and Inomata, Y.: Synergy between air pollution and urban meteorological changes through aerosol-radiation-diffusion feedback—A case study of Beijing in January, *Atmospheric Environment*, 171, 98–110, <https://doi.org/10.1016/j.atmosenv.2017.10.018>, 2017.
- 25 Kang, Y., Liu, M., Song, Y., Huang, X., Yao, H., Cai, X., Zhang, H., Kang, L., Liu, X., Yan, X., He, H., Zhang, Q., Shao, M., and Zhu, T.: High-resolution ammonia emissions inventories in China from 1980 to 2012, *Atmospheric Chemistry and Physics*, 16, 2043–2058, <https://doi.org/10.5194/acp-16-2043-2016>, 2016.
- Li, G., Bei, N., Cao, J., Huang, R., Wu, J., Feng, T., Wang, Y., Liu, S., Zhang, Q., Tie, X., and Molina, L.: A Possible Pathway for Rapid Growth of Sulfate during Haze Days in China, *Atmospheric Chemistry and Physics*, 17, 3301–3316, <https://doi.org/10.5194/acp-2016-994>, 2017a.
- 30 Li, K., Li, J., Wang, W., Tong, S., Liggio, J., and Ge, M.: Evaluating the effectiveness of joint emission control policies on the reduction of ambient VOCs: Implications from observation during the 2014 APEC summit in suburban Beijing, *Atmospheric Environment*, 164, 117–127, <https://doi.org/10.1016/j.atmosenv.2017.05.050>, 2017b.
- Li, M., Zhang, Q., Kurokawa, J. I., Woo, J. H., He, K., Lu, Z., Ohara, T., Song, Y., Streets, D. G., Carmichael, G. R., Cheng, Y., Hong, C., Huo, H., Jiang, X., Kang, S., Liu, F., Su, H., and Zheng, B.: MIX: A mosaic Asian anthropogenic emission inventory under the international collaboration framework of the MICS-Asia and HTAP, *Atmospheric Chemistry and Physics*, 17, 935–963, <https://doi.org/10.5194/acp-17-935-2017>, 2017c.





- Li, X., Zhang, Q., Zhang, Y., Zheng, B., Wang, K., Chen, Y., Wallington, T. J., Han, W., Shen, W., Zhang, X., and He, K.: Source contributions of urban PM<sub>2.5</sub> in the Beijing–Tianjin–Hebei region: Changes between 2006 and 2013 and relative impacts of emissions and meteorology, *Atmospheric Environment*, 123, 229–239, <https://doi.org/10.1016/j.atmosenv.2015.10.048>, 2015.
- Liang, P., Zhu, T., Fang, Y., Li, Y., Han, Y., Wu, Y., Hu, M., and Wang, J.: The Role of Meteorological Conditions and Pollution Control Strategies in Reducing Air Pollution in Beijing during APEC 2014 and Parade 2015, *Atmospheric Chemistry and Physics*, 2014, 1–62, <https://doi.org/10.5194/acp-2017-456>, 2017.
- Lin, Y.-L., Farley, R. D., and Orville, H. D.: Bulk Parameterization of the Snow Field in a Cloud Model, *Journal of Climate and Applied Meteorology*, 1983.
- Liu, H., Liu, C., Xie, Z., Li, Y., Huang, X., and Wang, S.: OPEN A paradox for air pollution controlling in China revealed by “ APEC Blue ” and “ Parade Blue ”, *Nature Publishing Group*, pp. 1–13, <https://doi.org/10.1038/srep34408>, 2016a.
- Liu, H., He, J., Guo, J., Miao, Y., Yin, J., Wang, Y., Xu, H., Liu, H., Yan, Y., Li, Y., and Zhai, P.: The blue skies in Beijing during APEC 2014 : A quantitative assessment of emission control efficiency and meteorological influence, *Atmospheric Environment*, 167, 235–244, <https://doi.org/10.1016/j.atmosenv.2017.08.032>, 2017.
- Liu, T., Gong, S., Yu, M., Zhao, Q., Li, H., He, J., Zhang, J., Li, L., Wang, X., Li, S., Lu, Y., Du, H., Wang, Y., Zhou, C., and Liu, H.: Attributions of meteorological and emission factors to the 2015 winter severe haze pollution episodes in Northern China, *Atmospheric Chemistry and Physics*, pp. 1–19, <https://doi.org/10.5194/acp-2016-798>, 2016b.
- Ma, J., Zhang, W., Xu, Y., Xie, H., Xu, X., Li, Q., Gao, J., Zheng, J., Xian, Z., Li, X., and Sheng, L., eds.: *China Statistical Yearbook*, China Statistics Publishing House, september edn., 2014.
- Mailler, S., Khvorostyanov, D., and Menut, L.: Impact of the vertical emission profiles on background gas-phase pollution simulated from the EMEP emissions over Europe, *Atmospheric Chemistry and Physics*, 13, 5987–5998, <https://doi.org/10.5194/acp-13-5987-2013>, 2013.
- Matsui, H., Koike, M., Kondo, Y., Takegawa, N., Kita, K., Miyazaki, Y., Hu, M., Chang, S. Y., Blake, D. R., Fast, J. D., Zaveri, R. A., Streets, D. G., Zhang, Q., and Zhu, T.: Spatial and temporal variations of aerosols around Beijing in summer 2006: Model evaluation and source apportionment, *Journal of Geophysical Research Atmospheres*, 114, 1–22, <https://doi.org/10.1029/2008JD010906>, 2009.
- Meng, R., Zhao, F. R., Sun, K., Zhang, R., Huang, C., Yang, J., Müller, R., and Thenkabail, P. S.: Analysis of the 2014 " APEC Blue " in Beijing Using More than One Decade of Satellite Observations: Lessons Learned from Radical Emission Control Measures, *Remote Sens*, 7, 15 224–15 243, <https://doi.org/10.3390/rs71115224>, 2014.
- Mlawer, E. J., Taubman, S. J., Brown, P. D., Iacono, M. J., and Clough, S. a.: Radiative transfer for inhomogeneous atmospheres: RRTM, a validated correlated-k model for the longwave, *Journal of Geophysical Research*, 102, 16 663, <https://doi.org/10.1029/97JD00237>, 1997.
- Monin, A. and Obukhov, A.: Basic laws of turbulent mixing in the surface layer of the atmosphere, *Contrib. Geophys. Inst. Acad. Sci. USSR*, 24, 163–187, 1954.
- Ng, N. L., Herndon, S. C., Trimborn, A., Canagaratna, M. R., Croteau, P. L., Onasch, T. B., Sueper, D., Worsnop, D. R., Zhang, Q., Sun, Y. L., and Jayne, J. T.: An Aerosol Chemical Speciation Monitor (ACSM) for Routine Monitoring of the Composition and Mass Concentrations of Ambient Aerosol, *Aerosol Science and Technology*, 45, 780–794, <https://doi.org/10.1080/02786826.2011.560211>, 2011.
- Pope, C. A., Ezzati, M., and Dockery, D. W.: Fine-Particulate Air Pollution and Life Expectancy in the United States, *New England Journal of Medicine*, 360, 376–386, <https://doi.org/10.1056/NEJMsa0805646>, 2009.
- Shang, X., Zhang, K., Meng, F., Wang, S., Lee, M., Suh, I., Kim, D., Jeon, K., Park, H., Wang, X., and Zhao, Y.: Characteristics and source apportionment of fine haze aerosol in Beijing during the winter of 2013, *Atmospheric Chemistry and Physics*, 18, 2573–2584, <https://doi.org/10.5194/acp-18-2573-2018>, 2018.



- Sun, Y., Wang, Z., Dong, H., Yang, T., Li, J., Pan, X., Chen, P., and Jayne, J. T.: Characterization of summer organic and inorganic aerosols in Beijing, China with an Aerosol Chemical Speciation Monitor, *Atmospheric Environment*, 51, 250–259, <https://doi.org/10.1016/J.ATMOENV.2012.01.013>, 2012.
- Sun, Y., Chen, C., Zhang, Y., Xu, W., Zhou, L., Cheng, X., Zheng, H., Ji, D., Li, J., Tang, X., Fu, P., and Wang, Z.: Rapid formation and evolution of an extreme haze episode in Northern China during winter 2015, *Sci Rep*, 6, 27 151, <https://doi.org/10.1038/srep27151>, 2016a.
- 5 Sun, Y., Wang, Z., Wild, O., Xu, W., Chen, C., Fu, P., Du, W., Zhou, L., Zhang, Q., Han, T., Wang, Q., Pan, X., Zheng, H., Li, J., Guo, X., Liu, J., and Worsnop, D. R.: “APEC Blue”: Secondary Aerosol Reductions from Emission Controls in Beijing, *Scientific Reports*, 6, 20 668, <https://doi.org/10.1038/srep20668>, 2016b.
- Tang, G., Zhu, X., Hu, B., Xin, J., Wang, L., Munkel, C., Mao, G., and Wang, Y.: Vertical variations of aerosols and the effects responded to the emission control: application of lidar ceilometer in Beijing during APEC, 2014, *Atmospheric Chemistry and Physics*, 15, 13 173–13 209, <https://doi.org/doi:10.5194/acp-15-12667-2015>, 2015.
- Tie, X., Zhang, Q., He, H., Cao, J., Han, S., Gao, Y., Li, X., and Jia, X. C.: A budget analysis of the formation of haze in Beijing, *Atmospheric Environment*, 100, 25–36, <https://doi.org/10.1016/j.atmosenv.2014.10.038>, 2014.
- Wang, G., Cheng, S., Wei, W., Yang, X., Wang, X., Jia, J., Lang, J., and Lv, Z.: Characteristics and emission-reduction measures evaluation of PM<sub>2.5</sub> during the two major events APEC and Parade, *Science of the Total Environment*, 595, 81–92, <https://doi.org/10.1016/j.scitotenv.2017.03.231>, 2017.
- 15 Wang, H., Zhao, L., Xie, Y., and Hu, Q.: “APEC blue”-The effects and implications of joint pollution prevention and control program, *Science of the Total Environment*, 553, 429–438, <https://doi.org/10.1016/j.scitotenv.2016.02.122>, 2016a.
- Wang, L. T., Wei, Z., Yang, J., Zhang, Y., Zhang, F. F., Su, J., Meng, C. C., and Zhang, Q.: The 2013 severe haze over southern Hebei, China: model evaluation, source apportionment, and policy implications, *Atmospheric Chemistry and Physics*, 14, 3151–3173, <https://doi.org/10.5194/acp-14-3151-2014>, 2014.
- 20 Wang, Y., Zhang, Y., Jay, J., Foy, B. D., Guo, B., and Zhang, Y.: Relative impact of emissions controls and meteorology on air pollution mitigation associated with the Asia-Pacific Economic Cooperation (APEC) conference in Beijing, China, *Science of the Total Environment*, 571, 1467–1476, <https://doi.org/10.1016/j.scitotenv.2016.06.215>, 2016b.
- 25 Wen, W., Cheng, S., Chen, X., Wang, G., and Li, S.: Impact of emission control on PM<sub>2.5</sub> and the chemical composition change in Beijing-Tianjin-Hebei during the APEC summit 2014, *Environmental Science and Pollution Research*, 23, 4509–4521, <https://doi.org/10.1007/s11356-015-5379-5>, 2016.
- Westervelt, D., Horowitz, L., Naik, V., Tai, A., Fiore, A., and Mauzerall, D.: Quantifying PM<sub>2.5</sub>-meteorology sensitivities in a global climate model, *Atmospheric Environment*, 142, 43–56, <https://doi.org/10.1016/J.ATMOENV.2016.07.040>, 2016.
- 30 Wiedinmyer, C., Akagi, S. K., Yokelson, R. J., Emmons, L. K., Al-Saadi, J. a., Orlando, J. J., and Soja, a. J.: The Fire INventory from NCAR (FINN): a high resolution global model to estimate the emissions from open burning, *Geoscientific Model Development*, 4, 625–641, <https://doi.org/10.5194/gmd-4-625-2011>, 2011.
- Wild, O., Zhu, X., and Prather, M. J.: Fast-J: Accurate simulation of in- and below-cloud photolysis in tropospheric chemical models, *Journal of Atmospheric Chemistry*, 37, 245–282, <https://doi.org/10.1023/A:1006415919030>, 2000.
- 35 Xu, W. Q., Sun, Y. L., Chen, C., Du, W., Han, T. T., Wang, Q. Q., Fu, P. Q., Wang, Z. F., Zhao, X. J., Zhou, L. B., Ji, D. S., Wang, P. C., and Worsnop, D. R.: Aerosol composition, oxidation properties, and sources in Beijing: results from the 2014 Asia-Pacific Economic Cooperation summit study, *Atmospheric Chemistry and Physics*, 15, 13 681–13 698, <https://doi.org/10.5194/acp-15-13681-2015>, 2015.



- Yan, D., Lei, Y., Shi, Y., Zhu, Q., Li, L., and Zhang, Z.: Evolution of the spatiotemporal pattern of PM<sub>2.5</sub> concentrations in China – A case study from the Beijing-Tianjin-Hebei region, *Atmospheric Environment*, 183, 225–233, <https://doi.org/10.1016/j.atmosenv.2018.03.041>, 2018.
- Yang, L., Wu, Y., Davis, J. M., and Hao, J.: Estimating the effects of meteorology on PM<sub>2.5</sub> reduction during the 2008 Summer Olympic Games in Beijing, China, *Frontiers of Environmental Science and Engineering in China*, 5, 331–341, <https://doi.org/10.1007/s11783-011-0307-5>, 2011.
- Yang, T., Wang, Z., Zhang, W., Gbaguidi, A., Sugimoto, N., Wang, X., and Matsui, I.: Technical note : Boundary layer height determination from lidar for improving air pollution episode modeling: development of new algorithm and evaluation, *Atmos. Chem. Phys.*, 17, 6215–6225, <https://doi.org/10.5194/acp-17-6215-2017>, 2017.
- 10 Zaveri, R. a. and Peters, L. K.: A new lumped structure photochemical mechanism for large-scale applications, *Journal of Geophysical Research*, 104, 30 387, <https://doi.org/10.1029/1999JD900876>, 1999.
- Zaveri, R. a., Easter, R. C., Fast, J. D., and Peters, L. K.: Model for Simulating Aerosol Interactions and Chemistry (MOSAIC), *Journal of Geophysical Research*, 113, D13 204, <https://doi.org/10.1029/2007JD008782>, 2008.
- Zhang, L., Wang, T., Lv, M., and Zhang, Q.: On the severe haze in Beijing during January 2013: Unraveling the effects of meteorological anomalies with WRF-Chem, *Atmospheric Environment*, 104, 11–21, <https://doi.org/10.1016/j.atmosenv.2015.01.001>, 2015.
- 15 Zhang, L., Shao, J., Lu, X., Zhao, Y., Hu, Y., Henze, D. K., Liao, H., Gong, S., and Zhang, Q.: Sources and Processes Affecting Fine Particulate Matter Pollution over North China: An Adjoint Analysis of the Beijing APEC Period, *Environmental Science and Technology*, 50, 8731–8740, <https://doi.org/10.1021/acs.est.6b03010>, 2016.
- Zhao, J., Du, W., Zhang, Y., Wang, Q., Chen, C., Xu, W., Han, T., Wang, Y., Fu, P., Wang, Z., Li, Z., and Sun, Y.: Insights into aerosol chemistry during the 2015 China victory day parade: results from simultaneous measurements at ground level and 260&thinsp;m in Beijing, *Atmospheric Chemistry and Physics*, pp. 3215–3232, <https://doi.org/10.5194/acp-2016-695>, 2017.
- 20 Zheng, B., Tong, D., Li, M., Liu, F., Hong, C., Geng, G., Li, H., Li, X., Peng, L., Qi, J., Yan, L., Zhang, Y., Zhao, H., Zheng, Y., He, K., and Zhang, Q.: Trends in China’s anthropogenic emissions since 2010 as the consequence of clean air actions, *Atmospheric Chemistry and Physics*, 2018, 1–27, <https://doi.org/10.5194/acp-2018-374>, 2018.
- 25 Zhong, J., Zhang, X., Dong, Y., Wang, Y., Liu, C., Wang, J., Zhang, Y., and Che, H.: Feedback effects of boundary-layer meteorological factors on cumulative explosive growth of PM<sub>2.5</sub> during winter heavy pollution episodes in Beijing from 2013 to 2016, *Atmospheric Chemistry and Physics*, 18, 247–258, <https://doi.org/10.5194/acp-18-247-2018>, 2018.
- Zhou, Y., Cheng, S., Lang, J., Chen, D., Zhao, B., Liu, C., Xu, R., and Li, T.: A comprehensive ammonia emission inventory with high-resolution and its evaluation in the Beijing-Tianjin-Hebei (BTH) region, China, *Atmospheric Environment*, 106, 305–317, <https://doi.org/10.1016/j.atmosenv.2015.01.069>, 2015.
- 30 Zhou, Y., Wang, Q., Huang, R., Liu, S., Tie, X., Su, X., Niu, X., Zhao, Z., Ni, H., Wang, M., Zhang, Y., and Cao, J.: Optical Properties of Aerosols and Implications for Radiative Effects in Beijing During the Asia-Pacific Economic Cooperation Summit 2014, *Journal of Geophysical Research: Atmospheres*, 122, 10,119–10,132, <https://doi.org/10.1002/2017JD026997>, 2017.